Supplementary materials

Paleowind Dire#ctions over the Tarim Block during the Mesoproterozoic, Northwestern China

Chenlin Hu, Changcheng Han, Jinghui Ma, Li Deng, and Lingfeng Zhao

Table S1. Location and sampling information for the eight study outcrops.

No.	Outcrop	Location	Thickness* (m)	No. analyses for anisotropy of magnetic susceptibility
1	QK (Qiakemaketieshi Outcrop)	41°25′ 22″ N; 87°49′ 08″ E	~3100 (BY-HG formations)	239
2	SW (Sawafuqi Outcrop)	41°44′ 51″ N; 79°47′ 42″ E	~2500 (QE-QG formations)	236
3	TK (Tiekelike Outcrop)	36°33′ 38″ N; 80°31′ 35″ E	~2700 (YL-KZ formations)	256
4	XG (Xingeer Outcrop)	41°28′ 36″ N; 88°44′ 30″ E	~3200 (BY-HG formations)	260
5	XY (Xiangyangcun Outcrop)	40°46′ 20″ N; 89°20′ 52″ E	~1900 (BY-HG formations)	254
6	XZ (Xinzanggonglu Outcrop)	37°52′ 58″ N; 77°24′ 49″ E	~2500 (YL-KZ formations)	255
7	YD (Yaerdangshan Outcrop)	40°43′ 46″ N; 89°00′ 18″ E	~1700 (BY-HG formations)	251
8	YM (Youermeinake Outcrop)	40°56′ 48″ N; 79°26′ 58″ E	~2600 (QE-QG formations)	251

*Total observed and measured thickness in a given outcrop. BY—Beiyixi Formation; HG—Hangeerqiaoke Formation; QE—Qiaoenbulake Formation; QG—Qigebulake Formation; YL—Yalaguzi Formation; KZ—Kezisuhumu Formation.

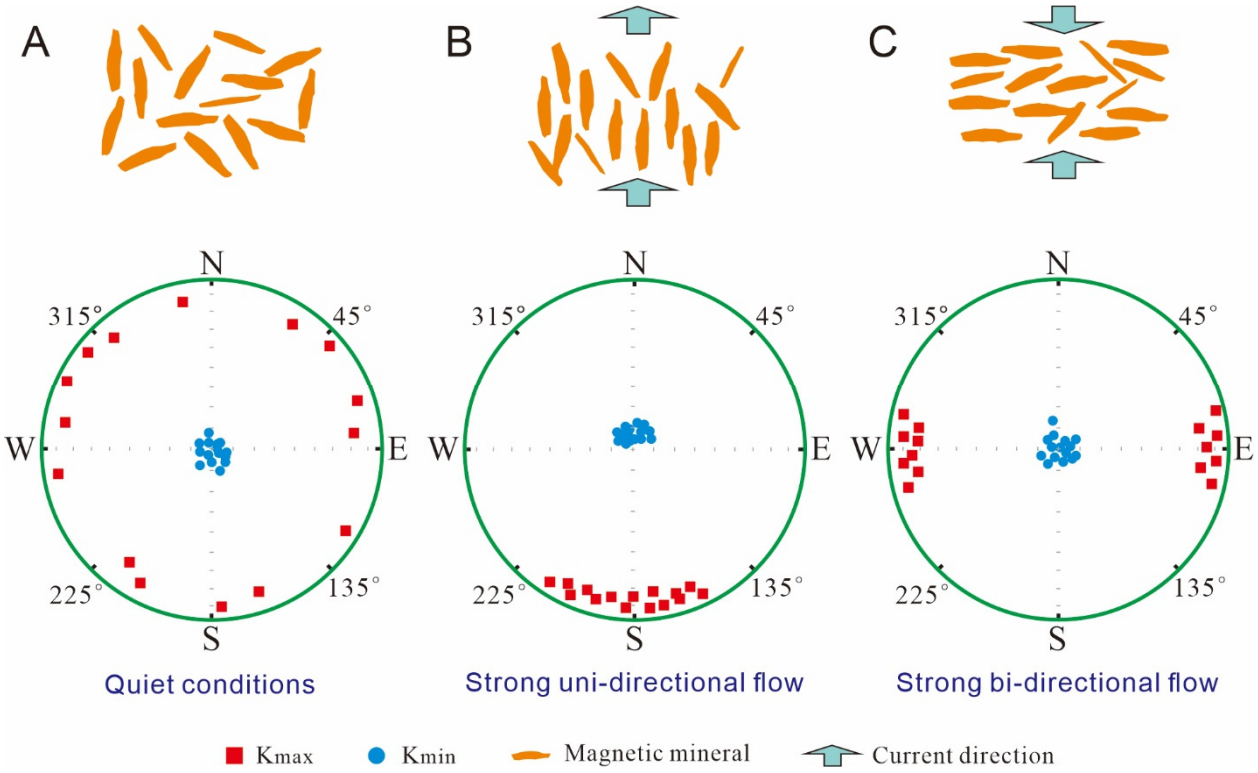

Figure S1. Theoretical depositional fabric in the presence of wind or water currents [1-3]. The orange grains illustrate the preferred alignment of most magnetic particles.

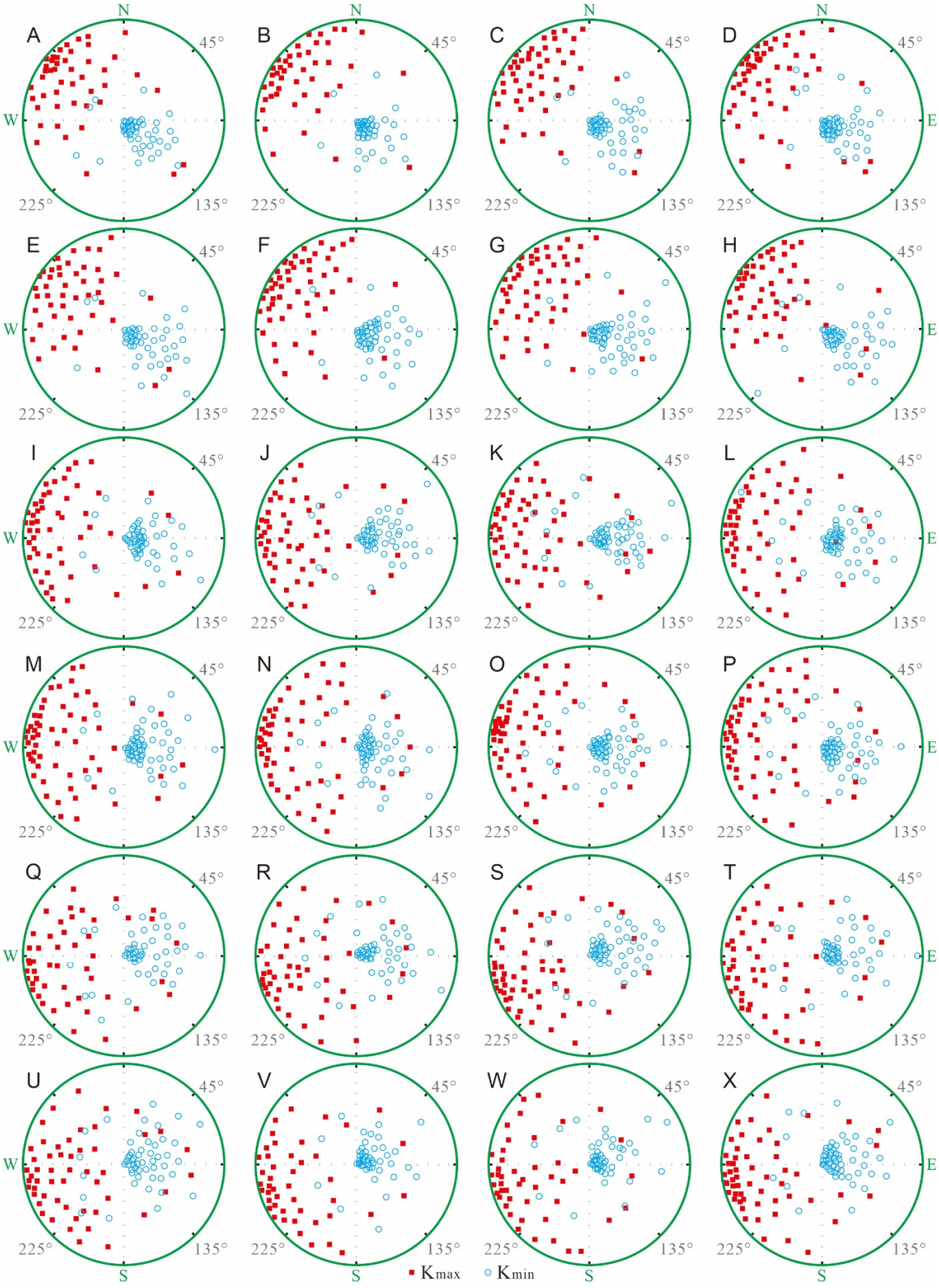
A
B
C
D
E
F
G
H
I
J
K
L
M
N
O
P
Q
R
S
T
U
V
W
X
N
S
W
E
45°
135°
225°
Kmax
Kmin

Figure S2. Equal-area projections (modern coordinates) of anisotropy of magnetic susceptibility principal axes of all samples for each Cryogenian series from the eight outcrops. (**A**) Lower Cryogenian at the QK Outcrop (n = 46). (**B**) Lower Cryogenian at the SW Outcrop (n = 44). (**C**) Lower Cryogenian at the TK Outcrop (n = 49). (**D**) Lower Cryogenian at the XG Outcrop (n = 51). (**E**) Lower Cryogenian at the XY Outcrop (n = 46). (**F**) Lower Cryogenian at the XZ Outcrop (n = 52). (**G**) Lower Cryogenian at the YD Outcrop (n = 52). (**H**) Lower Cryogenian at the YH Outcrop (n = 49). (**I**) Middle Cryogenian at the QK Outcrop (n = 51). (**J**) Middle Cryogenian at the SW Outcrop (n = 52). (**K**) Middle Cryogenian at the TK Outcrop (n = 55). (**L**) Middle Cryogenian at the XG Outcrop (n = 53). (**M**) Middle Cryogenian at the XY Outcrop (n = 57). (**N**) Middle Cryogenian at the XZ Outcrop (n = 55). (**O**) Middle Cryogenian at the YD Outcrop (n = 56). (**P**) Middle Cryogenian at the YM Outcrop (n = 56). (**Q**) Upper Cryogenian at the QK Outcrop (n = 48). (**R**) Upper Cryogenian at the SW Outcrop (n = 48). (**S**) Upper Cryogenian at the TK Outcrop (n = 54). (**T**) Upper Cryogenian at the XG Outcrop (n = 49). (**U**) Upper Cryogenian at the XY Outcrop (n = 52). (**V**) Upper Cryogenian at the XZ Outcrop (n = 45). (**W**) Upper Cryogenian at the YD Outcrop (n = 46). (**X**) Upper Cryogenian at the YM Outcrop (n = 55). K_{max}—maximum principal axes of the three-dimensional anisotropy of magnetic susceptibility ellipsoid; K_{min}—minimum principal axes of the three-dimensional anisotropy of magnetic susceptibility ellipsoid.

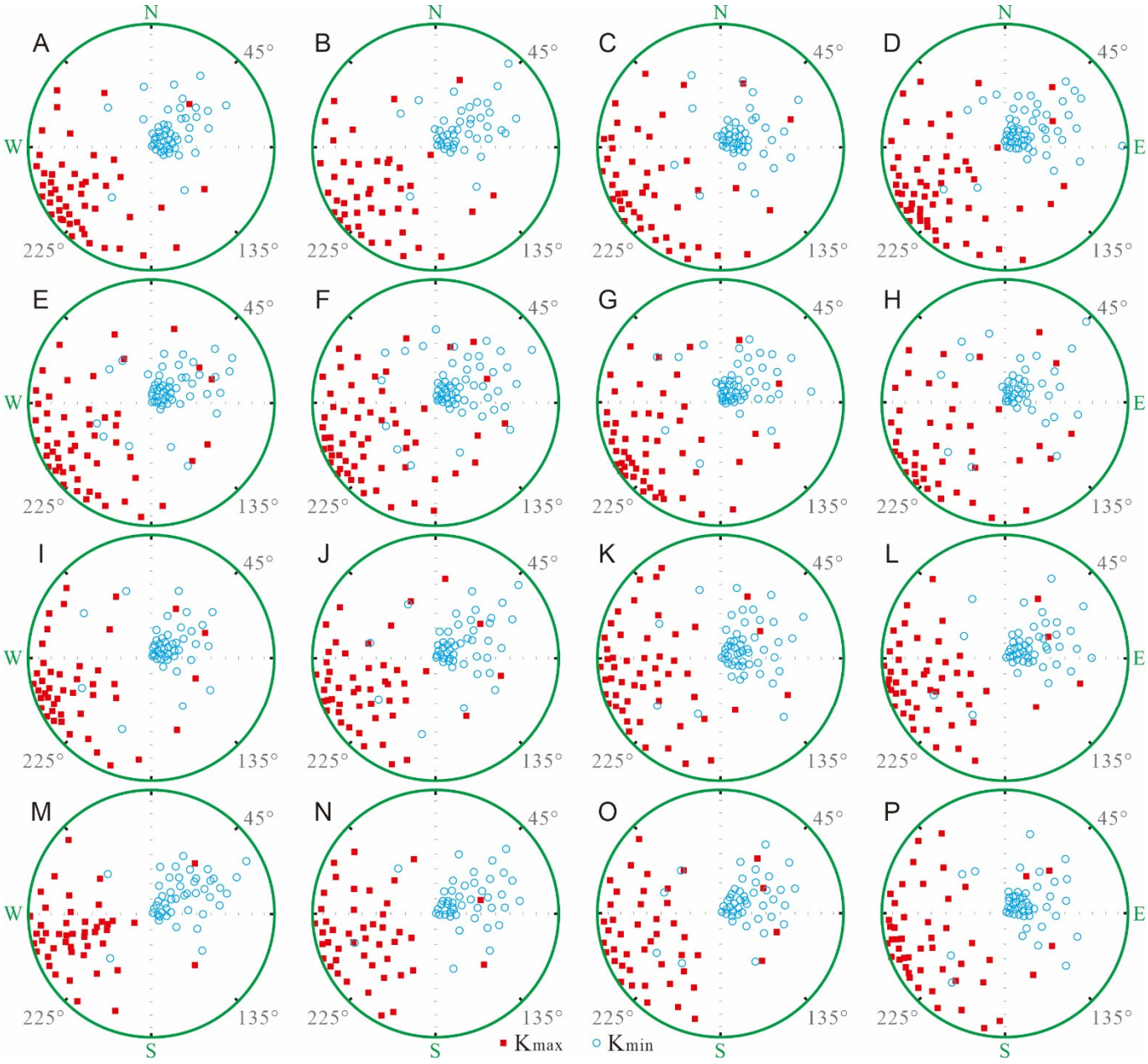

Figure S3. Equal-area projections (modern coordinates) of anisotropy of magnetic susceptibility principal axes of all samples for each Ediacaran series from the eight outcrops. (**A**) Lower Ediacaran at the QK Outcrop (n = 49). (**B**) Lower Ediacaran at the SW Outcrop (n = 44). (**C**) Lower Ediacaran at the TK Outcrop (n = 46). (**D**) Lower Ediacaran at the XG Outcrop (n = 57). (**E**) Lower Ediacaran at the XY Outcrop (n = 53). (**F**) Lower Ediacaran at the XZ Outcrop (n = 58). (**G**) Lower Ediacaran at the YD Outcrop (n = 52). (**H**) Lower Ediacaran at the YM Outcrop (n = 43). (**I**) Upper Ediacaran at the QK Outcrop (n = 45). (**J**) Upper Ediacaran at the SW Outcrop (n = 48). (**K**) Upper Ediacaran at the TK Outcrop (n = 52). (**L**) Upper Ediacaran at the XG Outcrop (n = 50). (**M**) Upper Ediacaran at the XY Outcrop (n = 46). (**N**) Upper Ediacaran at the XZ Outcrop (n = 45). (**O**) Upper Ediacaran at the YD Outcrop (n = 45). (**P**) Upper Ediacaran at the YM Outcrop (n = 48). K_{max}—maximum principal axes of the three-dimensional anisotropy of magnetic susceptibility ellipsoid; K_{min}—minimum principal axes of the three-dimensional anisotropy of magnetic susceptibility ellipsoid.

Supplemental references

1. Tarling, D.H.; Hrouda F. *The Magnetic Anisotropy of Rocks*; Chapman and Hall: London, UK, 1993; pp. 220.
2. Zhang, R.; Kravchinsky, V.A.; Zhu, R.; Yue, L. Paleomonsoon route reconstruction along a W–E transect in the Chinese Loess Plateau using the anisotropy of magnetic susceptibility: Summer monsoon model. *Earth Planet. Sc. Lett.* **2010**, *299*, 436-446. [CrossRef]
3. Zhu, R.; Liu, Q.; Jackson, M.J. Paleoenvironmental significance of the magnetic fab-rics in Chinese loess-paleosols since the last interglacial (< 130 ka). *Earth Planet. Sc. Lett.* **2004**, *221*, 55-69. [CrossRef]